https://doi.org/10.5194/hess-2023-29
Preprint. Discussion started: 21 March 2023

Hydrology and Earth System Sciences
Discussions
Open Access
EGU

Influence of bank slope on sinuosity-driven hyporheic exchange flow and residence time distribution during a dynamic flood event

Manuscript submitted to Hydrology and Earth System Sciences

Yiming Li[1,2], Uwe Schneidewind[2], Zhang Wen[1*], Stefan Krause[2], Hui Liu[1]

[1]Hubei Key Laboratory of Yangtze River Catchment Environmental Aquatic Science, School of Environmental Studies, China University of Geosciences, People's Republic of China

[2]School of Geography, Earth and Environmental Sciences, University of Birmingham, UK

***Correspondence:** Zhang Wen (wenz@cug.edu.cn)

https://doi.org/10.5194/hess-2023-29
Preprint. Discussion started: 21 March 2023

Hydrology and Earth System Sciences
Discussions
Open Access
EGU

Abstract. This study uses a reduced-order two-dimensional (2-D) horizontal model to investigate the influence of riverbank slope on the bank storage and sinuosity-driven hyporheic exchange flux (HEF) along sloping alluvial riverbanks during a transient flood event. The Deformed Geometry Method (DGM) is applied to quantify the displacement of the sediment-water interface (SWI) along the sloping riverbank during river stage fluctuation. This new model approach serves as the initial step to consider complicated floodplain morphologies in physics-based models for better predictions of HEF. Several controlling factors, including sinuosity, alluvial valley slope, and river flow advective forcing and duration of flow are incorporated in the model to investigate the effects of bank slope in aquifers of variable hydraulic transmissivity. Compared to simulations of a vertical riverbank, sloping riverbanks were found to increase the HEF. For sloping riverbanks, the hyporheic zone (HZ) encompassed a larger area and penetrated deeper into the alluvial aquifer, especially in aquifers with smaller transmissivity (i.e., larger aquifer hydraulic conductivity or smaller specific yield). Furthermore, consideration of sloping banks as compared to a vertical river bank can lead to both underestimation or overestimation of the pore water residence time. The impact of bank slope on residence time was more pronounced during a flood event for high transmissivity aquifer conditions, while it had a long-lasting influence after the flood event in lower transmissivity aquifers. Consequently, this decreases the residence time of HEF relative to the base flow condition. These findings highlight the need for (re)consideration of the importance of more complex riverbank morphology as control of hyporheic exchange in alluvial aquifers. The results have potential implications for river management and restoration and the management of river and groundwater pollution.

Key words: hyporheic exchange, sloping riverbank, transient river stage, peak flow event, residence time distribution

https://doi.org/10.5194/hess-2023-29
Preprint. Discussion started: 21 March 2023

Hydrology and Earth System Sciences
Discussions
Open Access
EGU

Nomenclature

ΔL	Nodal spacing [m]
∇	Laplace operator
α_L	Longitudinal dispersivity [L]
α_T	Transverse dispersivity [L]
D	Dispersion-diffusion tensor [L^2T^{-1}]
D_L	Water diffusivity [L^2T^{-1}]
J_x	Base groundwater gradient [-]
K	Hydraulic conductivity [LT^{-1}]
n	Scaling number [-]
n_0	Intensity of flood event [-]
n_d	Skewness of flood event [-]
S_y	Specific yield [-]
t_d	Duration of flood event [T]
t_p	Time to peak river stage [T]
α	Amplitude of the river boundary [L]
Γ_d	Dimensionless aquifer transmissivity [-]
δ	Bank slope angle [°]
δ_{ij}	Kronecker delta function [-]
ϵ	Tortuosity [-]
η	Degree of flood event asymmetry[T^{-1}]
θ	Effective porosity [-]
λ	River boundary wave length [L]
σ	River boundary sinuosity [-]
τ	Residence time [T]
ω	Flood event frequency[T^{-1}]
$h(\mathbf{x}, t)$	Transient groundwater head [L]
Δh^*	Dimensionless parameter of ambient groundwater flow [-]

https://doi.org/10.5194/hess-2023-29
Preprint. Discussion started: 21 March 2023

Hydrology and Earth System Sciences
Discussions

$A^{**}(t)$	Dimensionless variation of HZ area relative to base flow conditions [-]
$C(\mathbf{x}, t)$	Solute concentrations in the aquifer [ML^{-3}]
$C_0(\mathbf{x})$	Solute concentrations in initial condition [ML^{-3}]
$C_S(\mathbf{x}, t)$	Solute concentrations in the river [ML^{-3}]
$d^{**}(t)$	Dimensionless variation of HZ penetration distance relative to base flow conditions [-]
$H(\mathbf{x}, t)$	Thickness of the saturated aquifer [L]
$H_0(\mathbf{x})$	Initial river stage [L]
H_p	Peak river stage during the flood event [L]
$H_r(t)$	River stage at the downstream end [L]
$h_r(x, t)$	Transient river stage [L]
$M(t)$	Displacement of the sediment-water interface [L]
P_e	Péclet number [-]
$\mathbf{q}$	Specific discharge or Darcy flux [LT^{-1}]
$\mathbf{Q}$	Aquifer-integrated discharge [L^2T^{-1}]
$Q^*_{in,\,HZ}(t)$	Dimensionless net flux along the river boundary [-]
$Q^*_{in,\,HZ}(t)$	Dimensionless exchange flux from the aquifer to the river [-]
$Q^*_{out,\,HZ}(t)$	Dimensionless exchange flux from the river to the aquifer [-]
$Y(x, t)$	Location of the sediment-water interface boundary [L]
$z_b(\mathbf{x})$	Elevation of the underlying impermeable layer [L]
Γ_d	Dimensionless parameter of aquifer transmissivity [-]
$\mu(\mathbf{x}, 0)$	Mean (first order of) residence time distribution [T]
$\mu^*_{out}(x, t)$	Flux-weighted ratio of mean RT to mean RT under baseflow conditions [-]
$\mu_n(\mathbf{x}, t)$	n-th moment of residence time distribution [T^n]
$\mu_r^*(\mathbf{x}, t)$	Residence time distribution ratio between slope and vertical river bank model [-]
$\mu_{\tau 0\text{-max}}$	Maximum RT in the domain [T]

https://doi.org/10.5194/hess-2023-29
Preprint. Discussion started: 21 March 2023

Hydrology and Earth System Sciences
Discussions

$\mu_{\tau\text{-}S}(\mathbf{x}, t)$	Residence time distribution of slope river bank model [T]
$\mu_{\tau\text{-}V}(\mathbf{x}, 0)$	Residence time distribution of vertical river bank model [T]
$\rho(\mathbf{x}, t, \tau)$	Residence time distribution [T]

Abbreviations

HZ	Hyporheic zone
HEF	Hyporheic exchange flux
DGM	Deformed Geometry Method
SWI	Sediment-water interface
RTD	Residence time distribution
RT	Residence time
ALE	Arbitrary Lagrangian–Eulerian
2-D	Two-dimensional

43

44

https://doi.org/10.5194/hess-2023-29
Preprint. Discussion started: 21 March 2023

Hydrology and Earth System Sciences
Discussions
Open Access
EGU

1. Introduction

The hyporheic zone (HZ) can be described as the region that connects the river channel and adjacent aquifer, and includes riverbed and riverbanks. Mixing of different water types (groundwater, surface water) and ages in the HZ causes spatially and temporally varying exchange of water, biogeochemical species, and energy between river channel, riverbed and aquifer (Cardenas, 2009b; Hester and Gooseff, 2010; Krause et al., 2011, 2017, 2022; McClain et al., 2013; Boano et al., 2014). Hyporheic exchange flow in vertical (e.g., bedform-driven) and horizontal (e.g., meander-driven) domains can add to general regional groundwater upwelling or downwelling, with HEF representing those surface flow components that penetrate and transport through the hyporheic sediment and back into the stream. The distribution of hyporheic flow paths strongly determines the spatial and temporal distribution of biochemical characteristics of water within the riverbed and the wider river corridor as well as the formation of so-called hot zones and hot moments (Krause et al., 2013, 2017; Cardenas, 2015; Pinay et al., 2015).

Hyporheic exchange flux (HEF) is controlled by parameters such as stream discharge dynamics, recharge, riverbed and aquifer hydraulic properties, local pressure head fluctuations, and river geometry and morphology including sinuosity and riverbank slope (Larkin and Sharp, 1992; Gomez-Velez et al., 2012; 2017; Schmadel et al., 2016). For example, Cardenas et al. (2004) demonstrate how riverbed characteristics and especially heterogeneity could increase the hyporheic exchange intensity by 17% to 32%. As such, to be able to better estimate the relative importance of HEF on catchment water fluxes and biogeochemistry requires a good understanding of the interactions of its different drivers and controls. This is imperative as the spatiotemporal evolution of HEF paths, the resulting change in HZ extent (area) and thus also the mean residence time (RT) of the exchanged water in the HZ have significant impact on flow dynamics and transient storage along the river

https://doi.org/10.5194/hess-2023-29
Preprint. Discussion started: 21 March 2023


Hydrology and Earth System Sciences
Discussions

continuum and in turn control attenuation capacity (Weatherill et al., 2018) and biogeochemical functions of river corridors (Bertrand et al., 2012; Boulton et al., 2010; Brunke and Gonser, 1997).

Both lateral exchange between river and flood-plain, as well as bedform-induced vertical exchange at the streambed interface have been found to be crucial with regards to HEF and the biogeochemical transformation potential along the river corridor (Boano et al., 2010, 2014; Gomez-Velez and Harvey, 2014; Gomez-Velez et al., 2015, 2017; Kiel and Cardenas, 2014; Stonedahl et al., 2013). Considerable progress has been made in our understanding of how river planform geometry (Boano et al., 2006, 2010; Cardenas 2006; 2008; 2009a, 2009b; Stonedahl 2013), dynamic flood events (Gomez-Velez et al., 2012; 2017) and evapotranspiration (Kruegler et al., 2020) control HEF. Focusing on lateral exchange flow processes, Cardenas (2008; 2009a, 2009b) developed numerical models to investigate HEF and residence time distribution (RTD) for various river channel morphologies and regional groundwater flow conditions. Their simulations indicate that channel morphology, represented by sinuosity, is a dominant factor controlling HEF, the total HZ area, and RTD. In addition, Boano et al. (2010) used a similar modeling framework to study the relationship between RTD and biogeochemical transformation by introducing surface water as a major source of dissolved organic matter that triggers a sequence of redox reactions within the HZ. Reactive transport simulations showed a good relationship between RTD and denitrification reaction potential. Based on these studies, Gomez-Velez et al. (2012) conducted numerical simulations to investigate the impact of aquifer parameters (water table gradient, hydraulic conductivity, dispersivity) and channel sinuosity on HEF and RTD. By comparing RTD with the timescale of nitrate forming or reducing reactions, a meander can be classified as a source or sink of nitrate for (de)nitrification activities. More recent modeling studies have focused predominantly on the effects of dynamic river/groundwater stage fluctuations on lateral (e.g., Schmadel et al., 2016; Gomez-Velez et al., 2017) and vertical (e.g., Singh

https://doi.org/10.5194/hess-2023-29
Preprint. Discussion started: 21 March 2023


Hydrology and Earth System Sciences
Discussions

et al., 2019, 2020; Wu et al., 2018, 2020, 2021) hyporheic exchange and RTD. For example, Gomez-Velez et al. (2017) explored the HZ response to a dynamic river stage under different parameter values for hydraulic conductivity, river stage during flood events, groundwater gradient and river sinuosity conditions. Their results indicate that the dynamic forcing greatly influences net HEF, the area of HZ and RTD across different scenarios, whereby higher aquifer transmissivity will likely result in a stronger but shorter response of HEF and RTD to a flood event.

Although there is a considerable body of numerical research on the lateral hyporheic response to the various geometrical (e.g., geometry of river channel, river slope, etc) and dynamic drivers (e.g., fluctuation of river/groundwater, gaining and losing conditions of groundwater, etc), many HZ studies do not specifically consider floodplain-driven processes or they apply vertical riverbanks with straight river planimetry in an attempt to reduce model complexity in line with the analytical or numerical solutions used (Cooper and Rorabaugh, 1963; Hunt, 1990; Schmadel et al., 2016; Gomez-Velez et al., 2017;). However, riverbanks are usually tilted rather than vertical (Liang et al., 2018) as they undergo erosion (Osma and Thorne, 1988). Previous research has proven that bank erosion and bank collapse are globally spreading processes controlled by various factors, such as initial bank slope angle (Zingg, 1940; Lindow et al., 2009), surface flow forces (Hagerty et al., 1995; Fox and Wilson, 2010), vegetation cover (Mayor et al., 2008; Gao et al., 2009; Puttock et al., 2013) and sediment properties (Millar and Quich, 1993). Neglecting bank slope in analytical and numerical model solutions may therefore have a significant influence on the prediction accuracy of HEF (Doble et al. 2012a, 2012b) and RTD (Derx et al., 2014; Siergieiev et al., 2015). Thus, a detailed analysis of the floodplain drivers of HEF should require a more detailed consideration of the floodplain geometry including riverbank slope in bank storage conceptual models (Sharp, 1977).

Few previous studies have used numerical modeling where the model is bounded by a sloping riverbank to assess the influence of bank slope on HEF for a

https://doi.org/10.5194/hess-2023-29
Preprint. Discussion started: 21 March 2023


Hydrology and Earth System Sciences
Discussions

vertical section of an alluvial aquifer. In such cases, the aquifer was considered variably saturated, homogenous, and isotropic, while flow in the unsaturated zone was calculated using the Richards equation (Li et al., 2008; McCallum et al., 2010; Doble 2012a; b). These studies have confirmed that neglecting bank slope can lead to an underestimation of the bank storage volume as well as the temporal HEF in vertical cross-sectional profiles, especially under relatively small bank angles.

In turn, river sinuosity and ambient groundwater gradient (along the river channel) have not been studied as potential drivers of sinuosity-driven lateral HEF and RTD and their biogeochemical implications under complex riverbank morphological conditions and it needs to be determined whether considering both drivers can lead to significantly different findings as compared to previous cross-sectional profile models (Doble et al., 2012; Siergieiev et al., 2015; Derx et al., 2014). In this study, we therefore quantify the effect of bank slope on the simulated spatial extent (area) of the HZ in sinuosity-driven river meanders and how it impacts the evolution of HEF and RTD under varying aquifer transmissivity conditions to better understand lateral HEF through the alluvial plain. We build on the numerical model introduced by Gomez-Velez et al. (2017) and consider lateral bank slope by using a deformed geometry method (DGM) approach. For this, we couple DGM with the Boussinessq equation, the vertically integrated solute transport equation and residence time distribution equation to study HEF. Our results will help to reveal the importance of bank slope for the prediction of HEF and RTD in sinuosity-driven meandering rivers.

https://doi.org/10.5194/hess-2023-29
Preprint. Discussion started: 21 March 2023


Hydrology and Earth System Sciences
Discussions
Open Access
EGU

2. Methodology

2.1 Model setup with deformed geometry method

Our modeling approach builds on the work of Gomez-Velez et al. (2017), who developed a comprehensive simulation tool in dimensionless form that can represent most riverbank-aquifer situations and dynamic flood conditions. In our study, we use their model as a baseline with the same equations and metrics. Additional information regarding implementation of this baseline model can be found in the SI and Gomez-Velez et al. (2017). However, where Gomez-Velez et al. (2017) assume a vertical riverbank, we consider a sloping riverbank and use the DGM approach to capture the dynamic evolution of the SWI along the river course. A constant sloping angle (δ [°]) along the alluvial riverbank of a sinusoidal river was implemented in our model (see blue lines of conceptual model in Figure S1 and the corresponding mathematical model in Figure S2a) while the SWI was assumed to be always vertical (vertical solid red and green lines in Figure S2c). As such, the contraction or expansion of the simulated domain, i.e., displacement of the SWI can be characterized by the sloping angle (there is no movement of the SWI for the vertical riverbank case) and river stage. As the river stage changes, so does the location of the SWI.

When the river stage changes in our model, the sinusoidal boundary will migrate towards or away from the floodplain meaning that the submerged part of the riverbank is considered contracted and our model only considers the alluvial aquifer that is not submerged. The evolution of the SWI during a flood event can be calculated by considering river stage and bank slope via:

$$Y(x, t) = Y_0(x) + M(t) \quad (1)$$

where $Y(x, t)$ [L] is the location of the SWI boundary; $Y_0(x)$ [L] is the initial location of the SWI. In contrast to Gomez-Velez et al. (2017), the displacement of the SWI

https://doi.org/10.5194/hess-2023-29
Preprint. Discussion started: 21 March 2023


Hydrology and Earth System Sciences
Discussions
Open Access
EGU

caused by the deformation of the model domain ($M(t) = [h(t) - h(0)]/\tan(\delta)$, where $h(t)$ [L] is transient hydraulic head) is added in Eq. (1), which represents the displacement of the river boundary in y-direction due to river stage fluctuation and bank slope angle (see the horizontal distance between the vertical red and green solid line in Figure S2c).

To simulate the model domain deformation and mesh displacement, we use the DGM interface in COMSOL. In this interface, the deforming feature of a specified domain can be defined as a boundary condition with a given moving velocity or displacement. DGM is based on the arbitrary Lagrangian–Eulerian (ALE) method, which is a hybrid method that allows both the model domain and mesh to move or deform simultaneously in a predefined manner. More details on ALE can be found in Donea et al. (2014). While it has previously been used for simulating general free-surface problems (e.g., Duarte et al., 2004; Maury, 1996; Pohjoranta and Tenno, 2011), to our knowledge, DGM has not yet been implemented to solve moving boundary problems in hyporheic exchange studies. Here we used Eq. (1) as an input to the DGM interface to simulate the displacement of the SWI (water flow) during a dynamic flood event. Infiltration and seepage face before and after the peak time of the flood event, respectively, were neglected. Additionally, solute transport and RTD were simulated based on the extent of the flow field according to Gomez-Velez et al. (2017), as shown in the SI.

2.2 Model parameterization, testing and scenarios

Model hydraulic conditions used in our numerical modeling study are based on values from Gomez-Velez et al. (2017), who conducted a Monte Carlo analysis. They found that the dynamic variations of HEF and RTD are mainly determined by ambient groundwater flow (referred to as dimensionless parameter $\Delta h^* = \frac{J_x \lambda_2}{0.5(1+n_0)H_0}$, see Table 1) and the ratio of aquifer hydraulic conductivity to the duration of the flood event

https://doi.org/10.5194/hess-2023-29
Preprint. Discussion started: 21 March 2023

Hydrology and Earth System Sciences
Discussions
Open Access
EGU

(referred to as dimensionless constant $\Gamma_d = \frac{S_y \lambda_2}{0.5K(1+n_0)Hot_d}$, see Table 1). After setting up the original model of Gomez-Velez et al. (2017) as a baseline case (δ = 90°), we compared our model results for that case with those obtained by Gomez-Velez et al. (2017) for (a) net HEF represented by $Q^*_{net,\ HZ}(t)$; (b) area of HZ, $A^{**}(t)$; (c) penetration of the HZ, $d^*(t)$ in Γ_d = 0.1, 1, 10 and 100, and found that our model simulated those cases with high accuracy (Fig. 1). Parameters $A^{**}(t)$ and $d^*(t)$ are based on modeling the transport of a conservative solute while $Q^*_{net,\ HZ}(t)$ is based on modeling water flow. Slight differences between our model and that of Gomez-Velez et al. (2017) might be due to the use of a much more refined mesh in this study and different length scales.

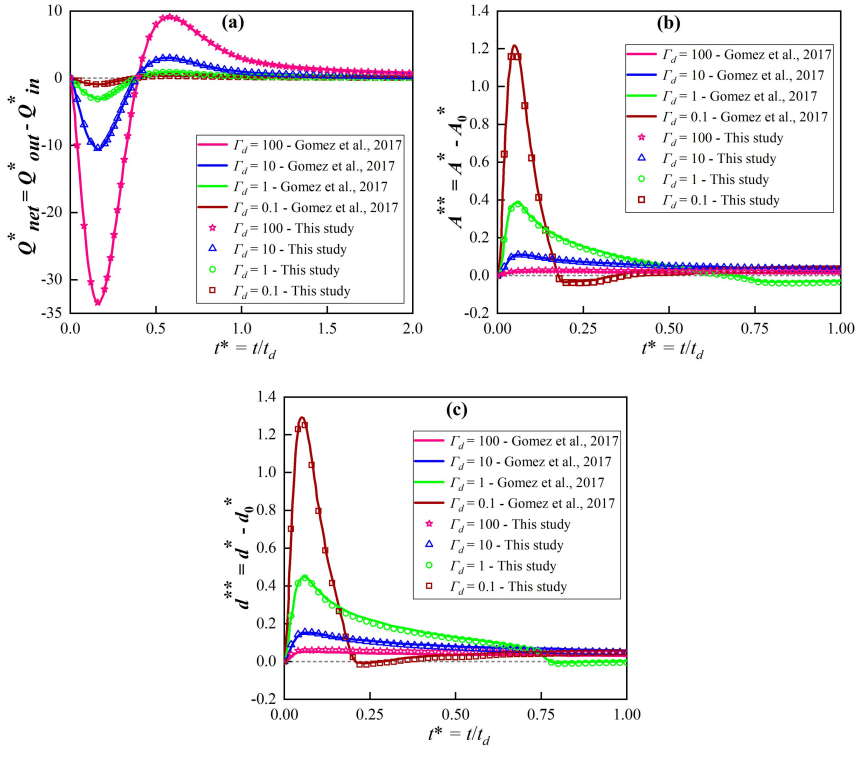

Figure 1. Comparison of results obtained in this study with those of Gomez et al. (2017) for the baseline case with a vertical river bank and variable Γ_d: (a) net

https://doi.org/10.5194/hess-2023-29
Preprint. Discussion started: 21 March 2023

Hydrology and Earth System Sciences
Discussions

hyporheic exchange flux represented by $Q^*_{net,\,HZ}(t)$; (b) extent of the hyporheic zone $A^{**}(t)$ and (c) penetration distance $d^*(t)$ of the hyporheic zone into the alluvial valley. A more refined mesh and different length scales used in this study, can explain occasional slight differences between our model and that of Gomez et al. (2017) might occur. Information regarding model fits can be found in the SI.

We then considered a series of riverbank scenarios where the bank slope angle ranged from $\delta = 90°$ (vertical riverbank) to 10° (nearly horizontal case) and Γ_d values ranged from 0.1 to 100, (corresponding to aquifer hydraulic conductivity ranging from 480 to 0.048 m/d, indicating high to low transmissivity. Table 1 presents the parameters used in our numerical modeling study. The finite-element models proposed in this study were developed using the COMSOL Multiphysics (COMSOL) software. Eq. (S1), Eq. (S3) and Eq. (S6) were implemented by customizing a PDE interface to include the Boussinessq, vertical integrated solute transport and RTD equation, respectively. The model domain was discretized into about 0.5 million variably-sized triangular elements, with refinement imposed near the river boundary. Mesh-independent numerical solutions are achieved by limiting grid size (ΔL) to less than 0.2 m. Thus, the transverse and longitudinal Peclet numbers (calculated by $P_e = \Delta L/\alpha_L$ and $P_e = \Delta L/\alpha_T$, respectively) in both advection and diffusion dominated zones are less than 1, which is smaller than the upper limit of $P_e = 4$ to effectively avoid numerical oscillations and instabilities.

Table 1. Parameters and values used in our numerical model simulations (adopted from Gomez-Velez et al. (2017)).

Parameters	Value	Description
Constant model parameters		
S_y	0.3	Specific yield [-]
λ	40	River boundary wave length [L]

https://doi.org/10.5194/hess-2023-29
Preprint. Discussion started: 21 March 2023

Hydrology and Earth System Sciences
Discussions

α	5	River boundary amplitude [L]
θ	0.3	Efficient porosity [-]
J_x	0.0025	Base groundwater gradient [-]
σ	1.14	River boundary sinuosity [-]
t_d	10	Duration of flood event [T]
n_d	0.25	Skewness of flood event [-]
t_p	$n_d t_d$	Time to peak river stage [T]
H_0	1	Base river stage [L]
n_0	1	Intensity of flood event [-]
α_L	2	Longitudinal dispersivity [L]
α_T	$0.1\alpha_L$	Transverse dispersivity [L]
Varied model parameters		
Γ_d	0.1 1 10 100	Dimensionless aquifer transmissivity [-]
δ	90 70 50 20 10	Bank slope angle [°]

241

242

https://doi.org/10.5194/hess-2023-29
Preprint. Discussion started: 21 March 2023

Hydrology and Earth System Sciences
Discussions
Open Access
EGU

3. Results

3.1 Effect of bank slope on hyporheic exchange flow and HZ patterns

3.1.1 Hyporheic exchange flow

The flow field (velocity magnitude and direction) and net HEF ($Q^*_{net,\ HZ}$ (t)) changed dynamically during and after the simulated flood event. Fig. 2a shows a comparison of $Q^*_{net,\ HZ}$ (t) values for different values of δ and Γ_d. In order to illustrate the influence of δ on $Q^*_{net,\ HZ}$ (t) under different Γ_d conditions more clearly, Fig. 2b - 2e highlight the $Q^*_{net,\ HZ}$ (t) evolution for a given Γ_d at smaller scale. Snapshots of the flow field and the boundary of the HZ area (isolines of $C(\mathbf{x}, t) = 0.5$ as concentration of a conservative solute) for different δ conditions at different times (pink dots in Fig. 2a) for $\Gamma_d = 1$ are shown in Fig. 3a - 3f.

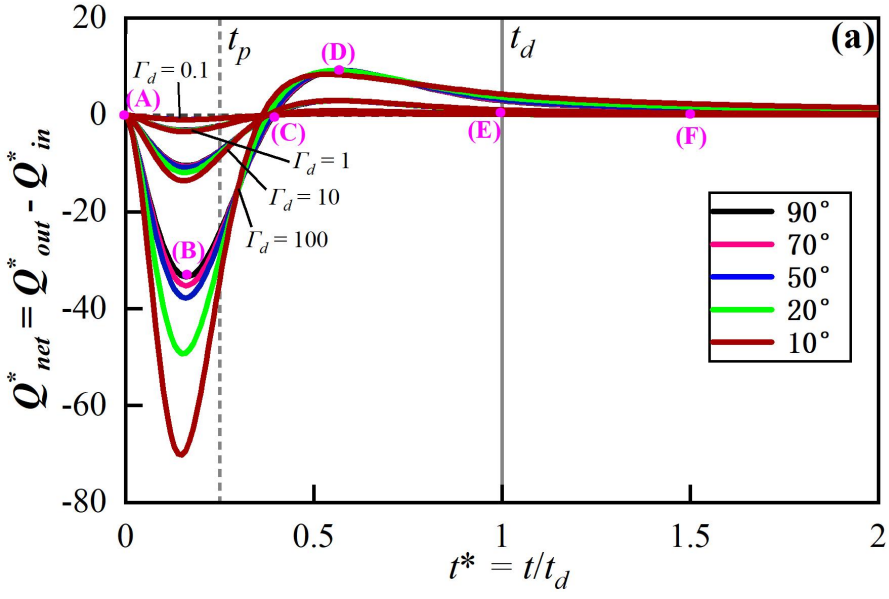

https://doi.org/10.5194/hess-2023-29
Preprint. Discussion started: 21 March 2023

Hydrology and Earth System Sciences
Discussions
Open Access
EGU

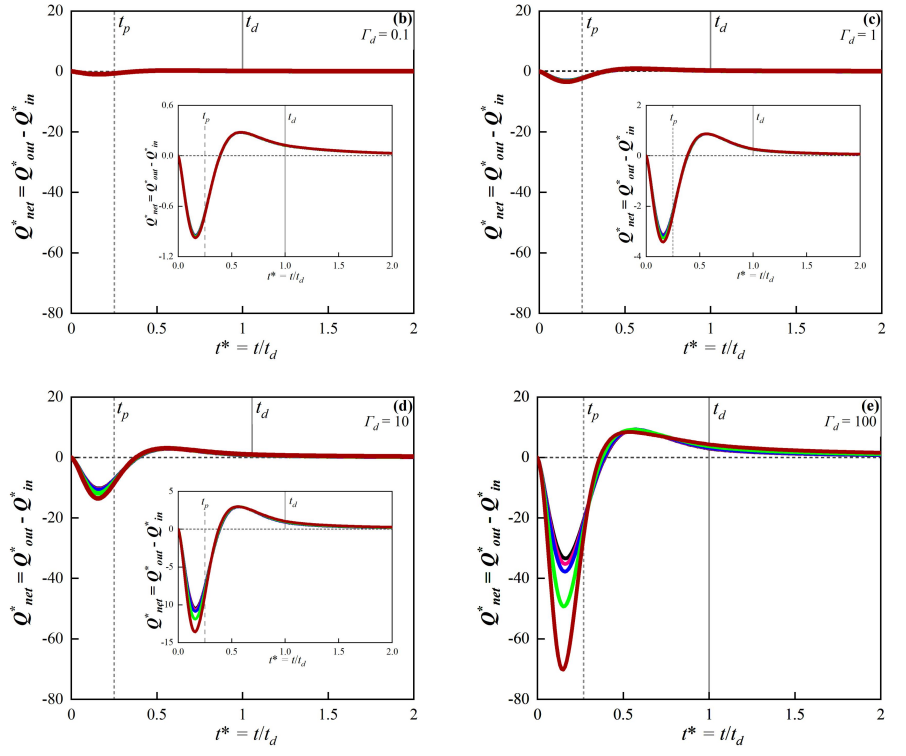

Figure 2. (a) Temporal evolution of dimensionless net flux for alternative values of Γ_d and δ (colored lines). The results for each Γ_d condition from 0.1 to 100 and different slopes are shown again in Fig. 2b - 2e separately, to represent smaller-scales. In each figure, time-to-peak (t_p) and flood duration (t_d) are marked by vertical dashed lines. Pink dots in (a) marked by (A) - (F) correspond to the snapshots of the flow field shown in Fig. 3. A negative flux value here represents water flow from river to aquifer.

https://doi.org/10.5194/hess-2023-29
Preprint. Discussion started: 21 March 2023

Hydrology and Earth System Sciences
Discussions
Open Access
EGU

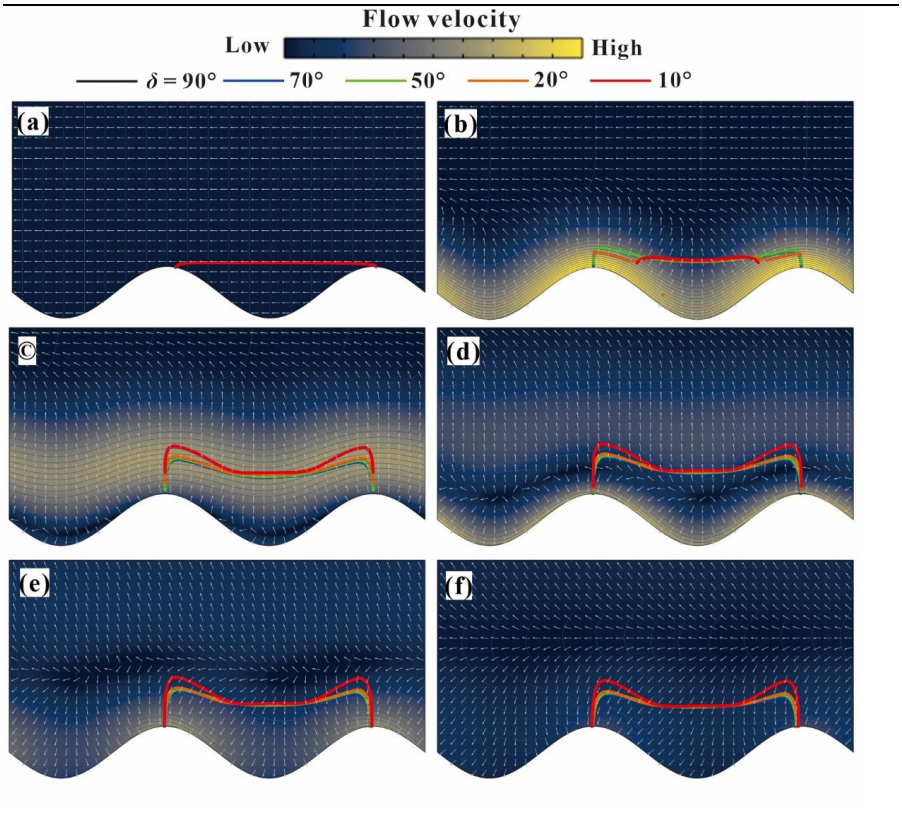

Figure 3. Temporal evolution of the alluvial flow field and spatial extent of the HZ. Snapshots of the flow field at different time steps during the simulated event (pink dots in Fig. 2a). Colored surfaces represent the magnitude of the Darcy flux vector (blue is low and yellow is high) and white isolines the dimensionless hydraulic head. Bold colored lines correspond to the HZ extent for different bank slope conditions.

Before the flood event (t = 0), steady state base flow conditions are assumed, as shown in Fig. 3a. The inflow and outflow (along the upstream and downstream meander bend, respectively) are in balance. The HZ boundaries for different δ conditions in Fig. 3a are the same before the flood event because the bank slope has no influence on the flow field and HZ extent. The onset of the flood event is indicated by the rising river stage and forces the river to infiltrate into the aquifer along the SWI (negative values of $Q^*_{net,\,HZ}$ (t) in Fig. 2), resulting in the expanded HZ as shown in

https://doi.org/10.5194/hess-2023-29
Preprint. Discussion started: 21 March 2023

Hydrology and Earth System Sciences
Discussions

Fig. 3b. The influx of river water into the HZ ($-Q^*_{net,\ HZ}\ (t)$) reaches its maximum before the time-to-peak river stage ($t = 0.25t_d$) because the pressure wave propagates into the aquifer and decreases the head gradient between the river and the connected aquifer. An aquifer with larger Γ_d limits the propagation of the pressure wave due to the low transmissivity, which leads to a larger head gradient near the SWI. This, consequently, leads to larger dimensionless net fluxes under increasing Γ_d conditions.

The maximum dimensionless flux ratios $Q^*_{max,\ var} = Q^*_{max,\ s}/\ Q^*_{max,\ v}$ of sloping ($\delta < 90°$, $Q^*_{max,\ s}$) and vertical ($\delta = 90°$, $Q^*_{max,\ v}$) riverbank cases are shown in Fig. 4. The bank slope is found to increase the infiltration flux by up to 120% ($Q^*_{max,\ var} \approx 2.2$) for $\Gamma_d = 100$ with $\delta = 10°$ while for larger slope angles or smaller Γ_d the dimensionless infiltration flux gradually decreases. This is because aquifers with smaller Γ_d (higher hydraulic transmissivity) are more sensitive to river stage variation and have a strong ability to transmit the pressure wave into the aquifer. In such cases, the influence of δ on the net flux becomes less important. On the other hand, a smaller δ induces a longer displacement of the SWI ($M(t)$) away from the river, where the groundwater head adjacent to the SWI is always relatively low (i.e., the head in base flow condition).

https://doi.org/10.5194/hess-2023-29
Preprint. Discussion started: 21 March 2023

Hydrology and Earth System Sciences
Discussions

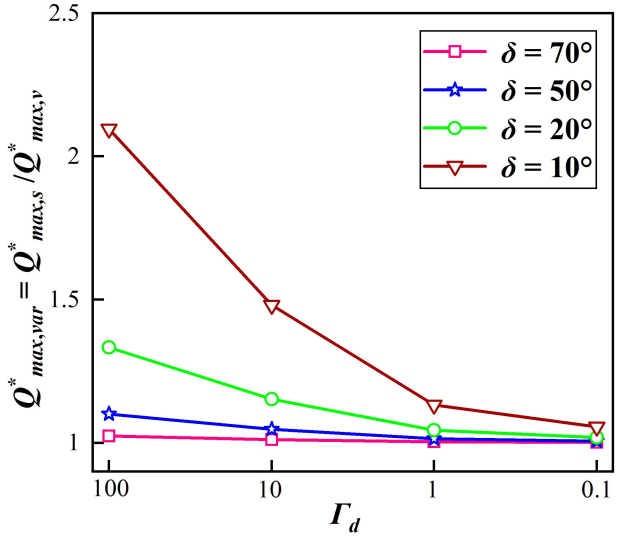

Figure 4. Ratio of maximum negative net flux of slope to no-slope (vertical river bank) conditions $Q^*_{max,var} = Q^*_{max,s}/Q^*_{max,}$ and aquifer transmissivities. The ratios of alternative slope condition are marked by different symbols and colors.

As the river stage decreases after t_p, the head gradient near the SWI gradually reverses and the net outflux starts increasing (the river is gaining water). This is associated with the river stage declining below the groundwater level (see Fig. 3c - 3f). Fig. 2 shows that the bank slope has little impact on the net outflux. Where $\Gamma_d = 100$, bank slope can slightly extend the time required for the system to recover to initial condition after t_p but in general, the response of the net outflux to bank slope is negligible when compared to that of the influx. Eventually, the net flux converges to zero, which indicates the flow field within the aquifer recovers to the initial conditions.

3.1.2 Patterns of hyporheic area and penetration distance

Fig. 5a and Fig. 6a show the temporal evolution of the HZ area ($A^{**}(t)$) and penetration distance ($d^{**}(t)$) into the alluvial valley relative to the initial condition for

https://doi.org/10.5194/hess-2023-29
Preprint. Discussion started: 21 March 2023

Hydrology and Earth System Sciences
Discussions

316 varying Γ_d and slope angles, while Fig. 5b – 5e and Fig. 6b – 6e illustrate the impact
317 of δ on $A^{**}(t)$ and $d^{**}(t)$ for different values of Γ_d in a close-up.

318

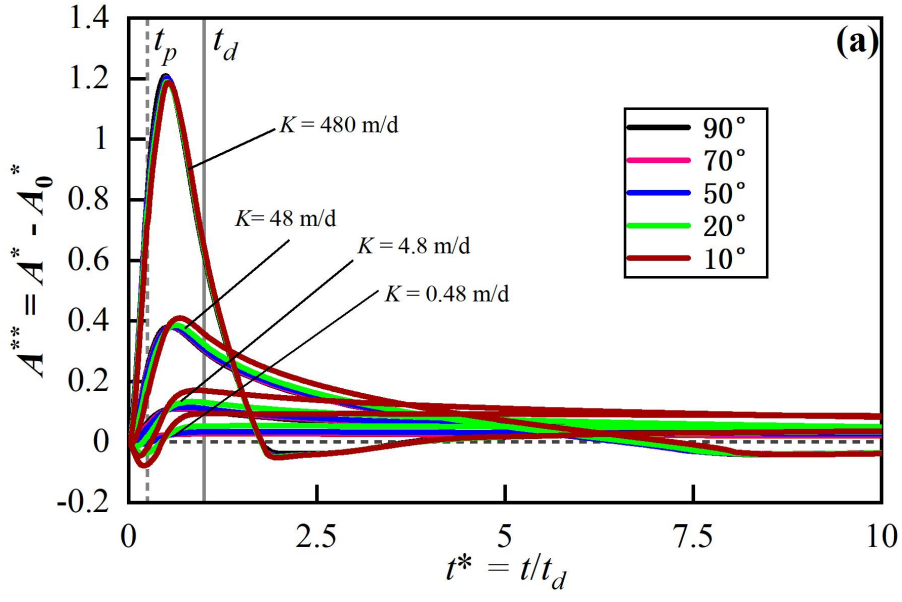

319

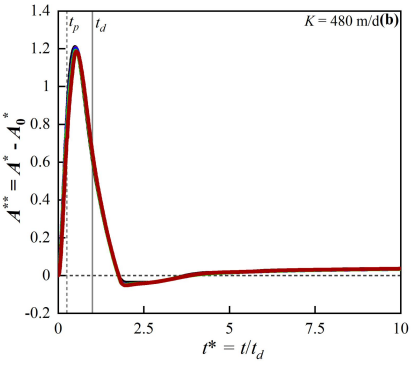

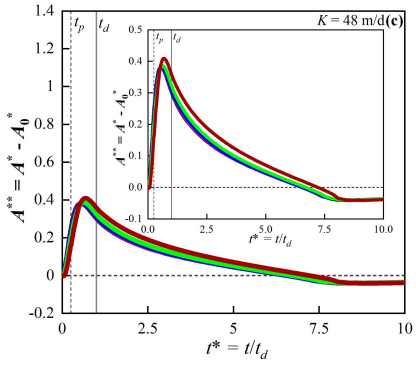

320

https://doi.org/10.5194/hess-2023-29
Preprint. Discussion started: 21 March 2023

Hydrology and Earth System Sciences
Discussions

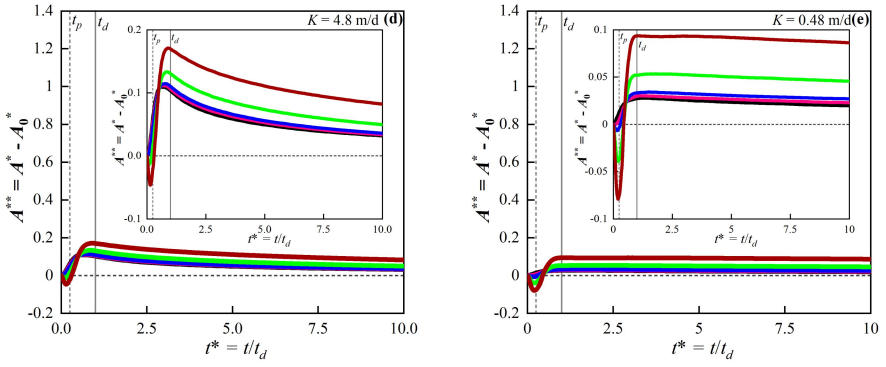

Figure 5. (a) Temporal evolution of HZ area for different values of Γ_d and δ (colored lines). For clarity, the results for each Γ_d condition from 0.1 to 100 are shown again separately in (b) to (e), with inserts representing smaller scales.

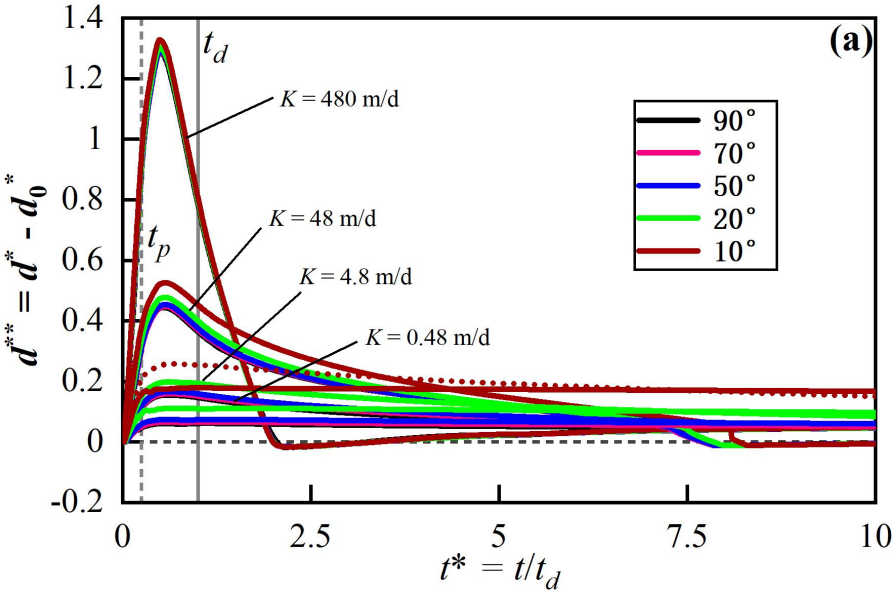

https://doi.org/10.5194/hess-2023-29
Preprint. Discussion started: 21 March 2023

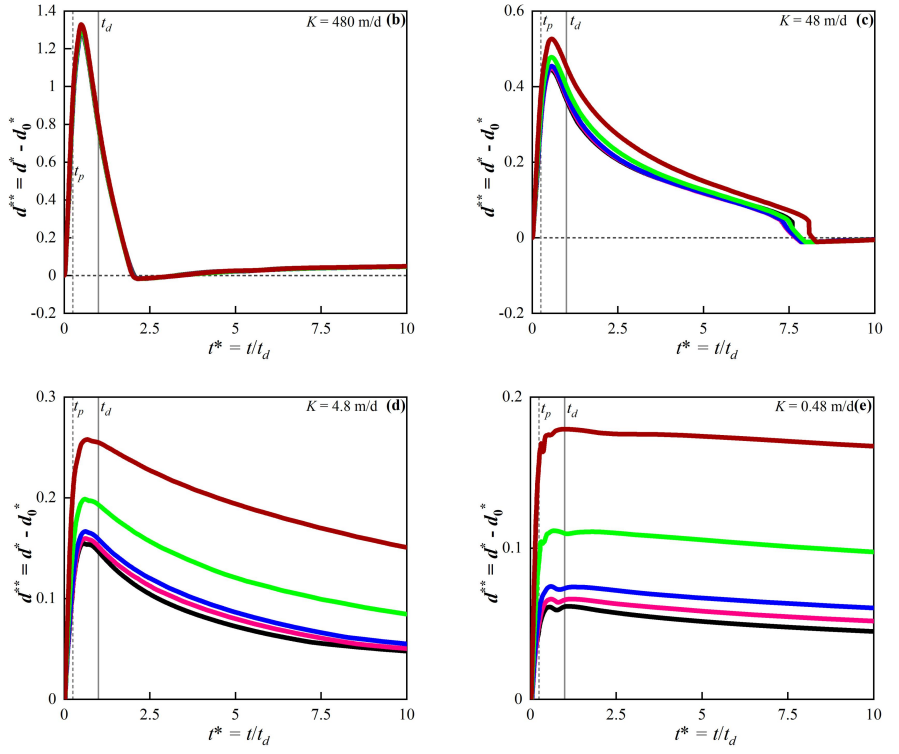

Figure 6. (a) Temporal evolution of HZ penetration distance into the alluvial valley for alternative values of Γ_d and δ (color lines). For clarity, the results for each Γ_d condition from 0.1 to 100 are shown again in (b) to (e), with inserts representing smaller scales.

For vertical banks ($\delta = 90°$, grey lines in Fig. 5), $A^{**}(t)$ increases synchronously with the river stage ($t < t_p$). After the peak time of the flood event ($t > t_p$), $A^{**}(t)$ continues to rise due to the water in the river still discharging into the aquifer. Furthermore, the groundwater mound continues to expand, migrating into the aquifer (see the more penetrated groundwater mound from in Fig. 3b vs Fig. 3c). After the flood event ($t > t_d$), the river water that was stored in the aquifer ($C(\mathbf{x}, t) > 0$) slowly discharges back into the river channel. Thus, the HZ area and penetration distance gradually rebound to initial conditions.

https://doi.org/10.5194/hess-2023-29
Preprint. Discussion started: 21 March 2023


Hydrology and Earth System Sciences
Discussions

Under sloping riverbank conditions, the riverbank will at times be submerged by the rising river stage. Fig. 5b and 6b show that the effects of bank slope on $A^{**}(t)$ and $d^{**}(t)$ are almost counteracted by the high transmissivity of the aquifer and the influence of bank slope on HZ area and penetration distance is negligible. At the beginning of the flood event, Fig. 5c - 5e show that for conditions with smaller δ, $A^{**}(t)$ can be less than zero (HZ at these times are smaller than the initial condition). This is due to the fact that the movement of the SWI during a rising river stage towards the alluvial valley will submerge parts that were previously unsaturated as the aquifer with low transmissivity will propagate water more slowly. As Γ_d increases from Fig. 5d - 5e, smaller values of A^{**} were observed that stay negative for a longer time for smaller bank slopes δ. This indicates that the bank slope has a more significant effect on HZ area in cases where Γ_d is large as a low-transmissivity aquifer takes more time to propagate infiltrating river water.

After about half of the flood duration ($t > 0.5t_d$), all of $A^{**}(t)$ becomes positive due to the re-emergence of the model domain submerged during the flood event. As Γ_d increases from Fig. 5b - 5e and from Fig. 6b - 6e, the impact of δ gradually emerges especially in larger Γ_d condition, whereby smaller δ can increase the peak values of $A^{**}(t)$ and $d^{**}(t)$, and delay the arrival time of the maximum value of $A^{**}(t)$. After the flood event ($t > t_d$), the effect of bank slope is counteracted by the higher aquifer transmissivity and only for large transmissivities has a significant impact on the HZ resulting in larger $A^{**}(t)$ and $d^{**}(t)$ as shown in Fig. 5c - 5e and Fig. 6c - 6e.

3.2 Spatiotemporal evolution of mean residence time distribution

The evolution of spatiotemporal patterns of mean RTD is a useful evaluation method for identifying the dynamic variation of aging and rejuvenation of hyporheic water. Here we use the mean RT ratio between a sloping model and a vertical model $\mu_r^*(\mathbf{x}, t) = \log_{10}(\mu_{\tau\text{-}S}(\mathbf{x}, t)/\mu_{\tau\text{-}V}(\mathbf{x}, 0))$ to evaluate the influence of bank slope on the predicted RTD for a given location and time. Fig. 7 presents RTDs for the initial

https://doi.org/10.5194/hess-2023-29
Preprint. Discussion started: 21 March 2023

Hydrology and Earth System Sciences
Discussions
Open Access
EGU

condition, where $\mu_{\tau 0\text{-max}}$ is the maximum RT in the domain. It can be seen that the isolines representing the RT are almost horizontal in the area extending from the river but RT near the upstream river bend is smaller than downstream because the initial flow direction is towards the negative direction of the x axis. Notably, $\mu(\mathbf{x}, 0)$ grows almost exponentially as y increases, and a positive correlation to Γ_d at a given location is observed.

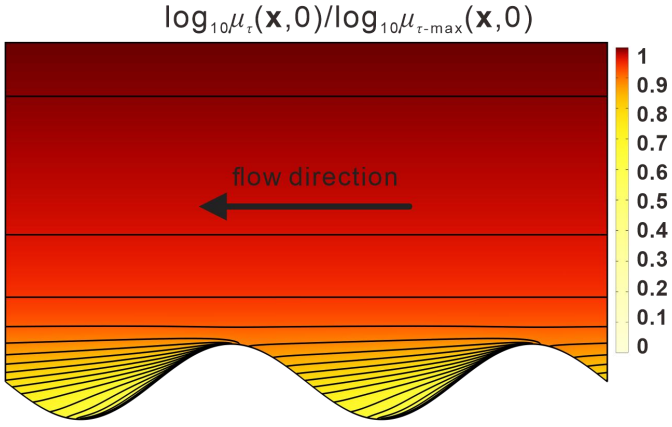

Figure 7. Relative mean residence time distributions [-] for baseline flow conditions (no slope), which are represented by $\log_{10}\mu_\tau(\mathbf{x}, 0)/\log_{10}\mu_{\tau\text{-max}}(\mathbf{x}, 0)$ to show the distribution pattern. The value of the contour lines grows exponentially with the distance from the river meander.

Fig. 8 - 11 present snapshots of μ_r^* for different bank slopes for Γ_d = 0.1, 1, 10 and 100, respectively, at the rising limb of the flood event (t/t_d = 0.1), the peak of flood event (t/t_d = 0.25), the falling limb of flood (t/t_d = 0.5) and after the flood event (t/t_d = 1, 2.5 and 10). The RT difference between sloping and vertical riverbank models are within 12.2% in the white-colored areas ($-0.05 < \mu_r^* < 0.05$) of Fig. 8 - 11, which indicates a minor effect of bank slope on RTD.

https://doi.org/10.5194/hess-2023-29
Preprint. Discussion started: 21 March 2023

Hydrology and Earth System Sciences
Discussions

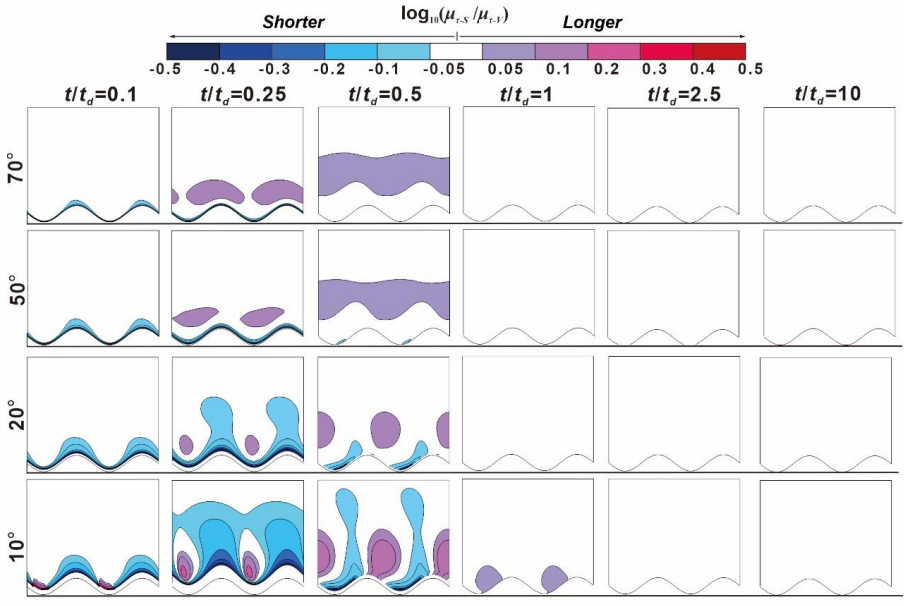

Figure 8. Snapshots for the RTD ratio $\mu_r^*(\mathbf{x}, t)$ between sloping and vertical riverbank conditions at different times t/t_d as a function of δ for Γ_d = 0.1. The horizontal lines beneath each figure are the reference lines to show the initial location of SWI. The lower sinuous lines at the reference lines are the initial SWIs.

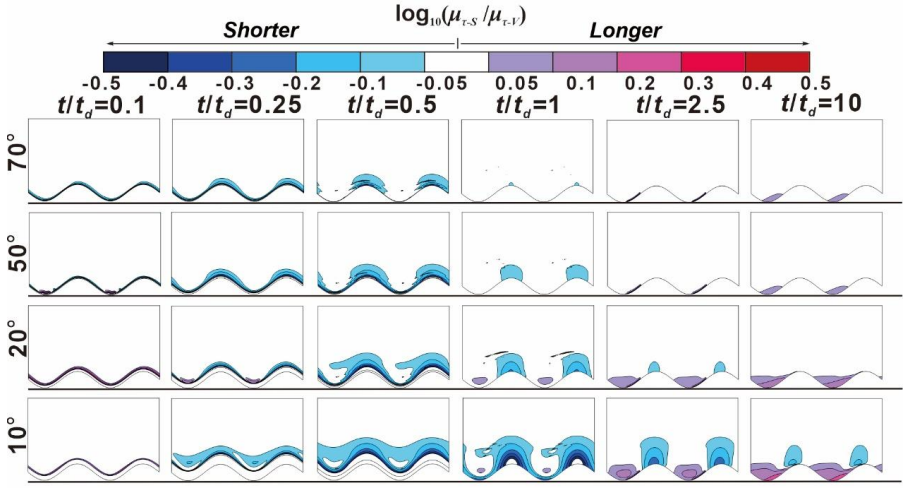

Figure 9. Snapshots for the RTD ratio $\mu_r^*(\mathbf{x}, t)$ between sloping and vertical riverbank conditions at different times t/t_d as a function of δ for Γ_d = 1. The horizontal lines

https://doi.org/10.5194/hess-2023-29
Preprint. Discussion started: 21 March 2023

Hydrology and Earth System Sciences
Discussions
Open Access
EGU

beneath each figure are the reference lines to show the initial location of SWI. The lower sinuous lines at the reference lines are the initial SWIs.

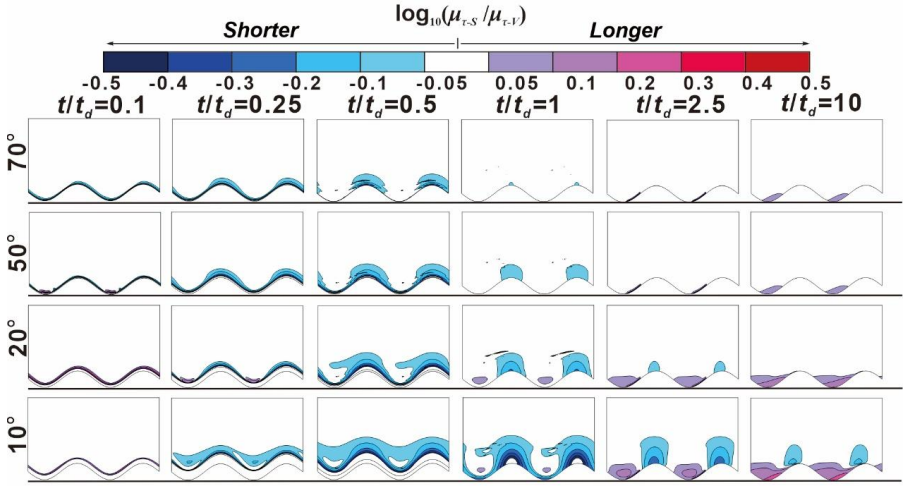

Figure 10. Snapshots for the RTD ratio $\mu_r^*(\mathbf{x}, t)$ between sloping and vertical riverbank conditions at different times t/t_d as a function of δ for Γ_d = 10. The horizontal lines beneath each figure are the reference lines to show the initial location of SWI. The lower sinuous lines at the reference lines are the initial SWIs.

https://doi.org/10.5194/hess-2023-29
Preprint. Discussion started: 21 March 2023

Hydrology and Earth System Sciences
Discussions
Open Access
EGU

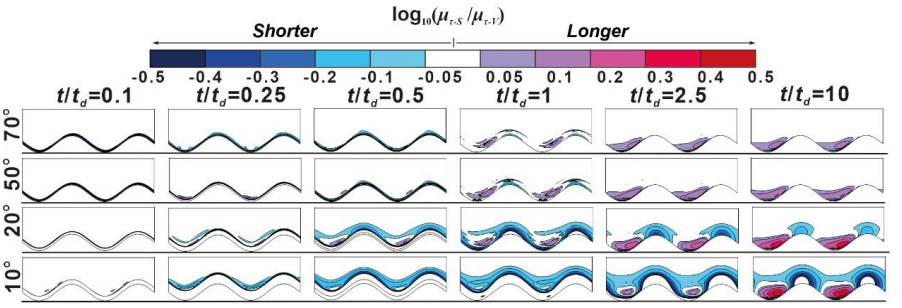

Figure 11. Snapshots for the RTD ratio $\mu_r^*(\mathbf{x}, t)$ between sloping and vertical riverbank conditions at different times t/t_d as a function of δ for Γ_d = 100. The horizontal lines beneath each figure are the reference lines to show the initial location of SWI. The lower sinuous lines at the reference lines are the initial SWIs.

At t/t_d = 0.1, a smaller bank slope can lead to shorter RT (negative values of μ_r^*) near the SWI. The area of shorter RT caused by bank slope was positively related to aquifer transmissivity. The effect of δ is small for Γ_d = 10 and 100 because the groundwater mound piles up around the river boundary, but that small area extended deeper into the alluvial valley for smaller δ. Due to the scattered and nested flow paths near the inner bend (cut bank) and outer bend (point bar), respectively, the penetration distance of the negative value of μ_r^*area at the cut bank of SWI is larger than that at the point bar. The change of flow direction near the point bar leads to a prolonged flow path for the water in the river as well as to forced groundwater mixing with the slightly older water. This effect was amplified with decreasing bank slope, but it is only statistically significant ($\mu_r^* < -0.05$ or $\mu_r^* > 0.05$) when $\delta = 10°$ at t/t_d = 0.1.

At the time of peak flood (t/t_d = 0.25), the river still infiltrates into the aquifer. For Γ_d = 0.1, bank slope can lead to both younger and older water, i.e., water undergoing shorter and longer RT. Both magnitude of μ_r^* and associated RT area increase with decreasing slope due to the longer penetration distance of river water

https://doi.org/10.5194/hess-2023-29
Preprint. Discussion started: 21 March 2023


Hydrology and Earth System Sciences
Discussions

into the aquifer. As δ decreases, the positive values of μ_r^* are located closer to the downstream point bar. The impact of bank slope on RTD for $\Gamma_d = 1$ is rather similar in its pattern compared to $\Gamma_d = 0.1$, but μ_r^* was significant only for $\delta = 10°$. For $\Gamma_d = 10$ and 100, the effect of bank slope can lead to larger and deeper penetration of the river water into the alluvial valley (Fig. 8 - 11) but this effect is smaller than when looking at smaller Γ_d because of the lower hydraulic transmissivity.

At $t/t_d = 0.5$, part of the submerged aquifer at $t/t_d = 0.25$ reemerges due to the decline in river stage. In most cases, smaller bank slopes can lead to wider reemergence of the aquifer, and therefore result in smaller μ_r^* near the river boundary; however, this is not the case for $\Gamma_d = 0.1$ where bank slope can both increase and decrease the RT of pore water. Furthermore, compared to when $t/t_d = 0.25$, the impact of bank slope becomes weaker for $\Gamma_d = 0.1$, but more relevant for the larger Γ_d values.

After the flood event ($t/t_d > 1$), the influence of bank slope on RT is nearly eliminated for $\Gamma_d = 0.1$ and 1 due to the high aquifer transmissivity. However, for aquifers with lower transmissivity ($\Gamma_d = 10$ and 100), bank slope still has a significant effect on RT at $t/t_d = 10$ and leads to older water near the point bar, which indicates the bank slope has a more lasting influence on aquifer RT, as more time is required to recover to initial condition.

3.3 Relative flux-weighted residence time

Fig. 12 shows the evolution of the flux-weighted relative RT $\mu^*_{out}(x, t) = \mathbf{n} \cdot Q^*_{out}(x, t) \log_{10}(\mu_r(x, t)/\mu_r(x, 0))$ for different slopes and aquifer transmissivities. $\mu^*_{out}(x, t)$ represents the difference in flux-weighted RT of the water discharged into the river compared to the initial condition. At the start of the flood event, there is no μ^*_{out} as river water infiltrates the aquifer. Following the decline in river stage, the aquifer begins to discharge the mixed water with different RT back into the river (see Fig. 3c).

https://doi.org/10.5194/hess-2023-29
Preprint. Discussion started: 21 March 2023

Hydrology and Earth System Sciences
Discussions

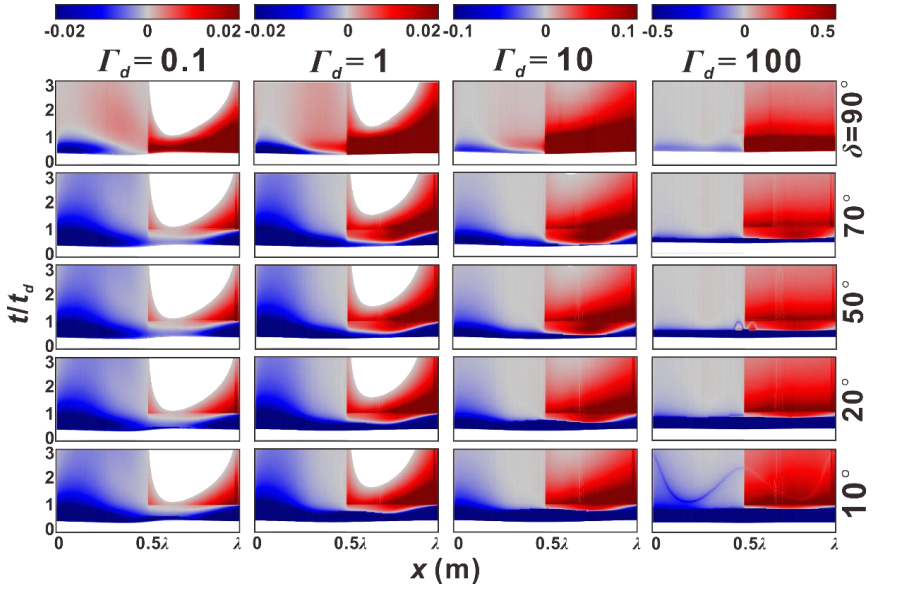

Figure 12. Temporal evolution of flux-weighted ratios of RT to the RT for base flow condition ($\mu^*_{out}(x, t) = \mathbf{n}\cdot Q^*_{out}(x, t)\log_{10}(\mu_\tau(x, t)/\mu_\tau(x, 0))$) along the river meander as a function of δ and Γ_d.

For vertical riverbank conditions (δ = 90°, top row in Fig. 12), upstream ($0.5\lambda < x < \lambda$) and downstream ($0 < x < 0.5\lambda$) boundaries of the meander bend discharge older and younger water, respectively. The waters with relatively younger or older RT are mostly discharged before the flood event ($t/t_d < 1$) due to the greater outflux as shown in Fig. 2a. It also can be seen that water is older along the upstream bend compared to the more rejuvenated water along the downstream bend. After the flood event, μ^*_{out} gradually disappears along the upstream meander (blank areas) for Γ_d = 0.1 and 1, because the flow fields are recovering to base flow conditions. Therefore, the upstream meander gradually becomes the inflow boundary.

For cases with lower values of Γ_d (left columns in Fig. 12), μ^*_{out} reaches equilibrium earlier compared to cases with higher Γ_d . As δ decreases from the top row to the bottom row in Fig. 12, the increased impact of bank slope causes μ^*_{out} to gradually decrease the RT of the outflux during the flood event. For larger Γ_d, μ^*_{out} is

https://doi.org/10.5194/hess-2023-29
Preprint. Discussion started: 21 March 2023


Hydrology and Earth System Sciences
Discussions

474 totally dominated by younger water during the flood event. Furthermore, the stronger
475 impact of smaller bank slope angles can both extend the time over which and increase
476 the magnitude with which younger water is discharging along the downstream
477 meander.

478 4. Discussion

479 4.1. Why we should account for bank slope

480 Tilted riverbanks are common in nature and caused by erosion and bank collapse,
481 as has been observed at multiple scales (Zingg, 1940). Previous studies have shown
482 that bank erosion is stronger where the river planimetry is more sinuous, river stage
483 varies more frequently, or where the riverbank has larger sloping angles, ultimately
484 leading to a flatter bank (Zingg. 1940; Hagorty et al., 1995; Mayor et al., 2008;
485 Puttock et al., 2013). Hence, recent studies have recognized the need for a
486 comprehensive analysis of how riverbank topography affects lateral hyporheic
487 exchange along meandering streams (Boano et al., 2014) and the specific importance
488 of bank slope on hyporheic exchange has been highlighted by Doble et al. (2012) and
489 Liang et al. (2018). Yet, in most previous studies, the impact of riverbank geometry
490 and in particular bank slope on sinuosity-driven lateral hyporheic exchange was
491 ignored. Flow was usually only considered perpendicular to the river axis, i.e., HEF in
492 river flow direction caused by the alluvial valley slope and river sinuosity was not
493 considered. However, as river planimetry can vary significantly along river corridors
494 (Hooke, 2013; Seminara, 2006), and the alluvial valley slope has a potentially
495 non-negligible impact on hyporheic exchange (Gomez-Velez et al., 2017), we
496 considered it important to close this knowledge gap by specifically focusing on the
497 impact of bank slope and the ambient groundwater gradient for various groundwater
498 flow conditions (as manifested through aquifer transmissivity) on HEF. Our results

https://doi.org/10.5194/hess-2023-29
Preprint. Discussion started: 21 March 2023


Hydrology and Earth System Sciences
Discussions

499 clearly indicate that HZ characteristics (flow field, area and penetration distance of
500 HZ into alluvial valley) can significantly vary along a meandering river depending on
501 bank slope conditions.

502 Not accounting for bank slope and river sinuosity can lead to an
503 underestimation of infiltration from the river to the alluvial aquifer. This effect is
504 more pronounced for smaller bank slope angles and losing conditions can be
505 significantly underestimated. Doble et al. (2012), Siergieiev et al. (2015) and Liang et
506 al. (2018), assessed the influence of bank slope on HEF using a vertical
507 cross-sectional profile. Siergieiev et al. (2015) found that the impact of bank slope on
508 HEF was proportional to the hydraulic conductivity of the aquifer. However, we argue
509 here that bank slope is more relevant in rivers connected to aquifers with low
510 hydraulic transmissivity. Furthermore, we show (Fig. 13) that using only one
511 cross-sectional river profile perpendicular to the river axis does not capture the effect
512 of river sinuosity on HEF as bank storage decreases from point bar to cut bank. That
513 means the previous vertical cross-sectional profile models could not calculate the
514 bank storage evolution accurately when neglecting the sinuosity of river. In a
515 meandering river with variable bank slope, river geometry thus has a sizable effect on
516 bank storage evolution and HEF, and should be included into the future analytical/
517 numerical models.
518

https://doi.org/10.5194/hess-2023-29
Preprint. Discussion started: 21 March 2023

Hydrology and Earth System Sciences
Discussions
Open Access
EGU

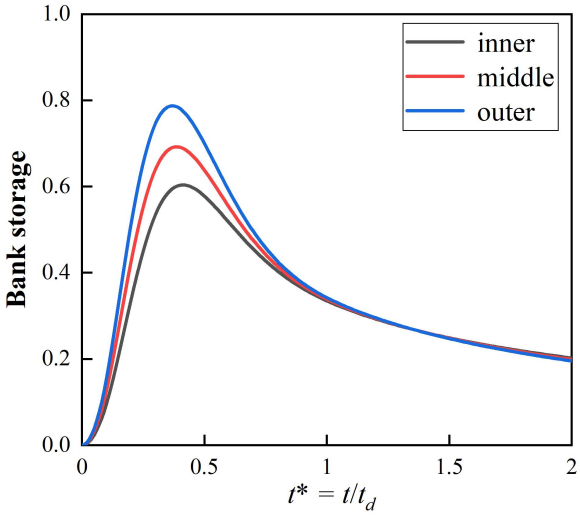

519

520 **Figure 13.** Bank storage versus time for $\Gamma_d = 1$ and $\delta = 90°$ condition at: inner bend
521 ($x = 0$); middle bend ($x = 0.25\lambda$); outer bend ($x = 0.25\lambda$). Dimensionless bank storage
522 was calculated by $\frac{\int_{Y(x,t)}^{Y(x,t)+4\lambda}[h\text{-}z_b\text{-}H_0]\mathrm{d}y}{\lambda H_p}$.

523

524 The impact of bank slope on RT is basically controlled by aquifer transmissivity.
525 When aquifer transmissivity increases, the impact of bank slope appears to be more
526 pronounced when river stage rises during a flood event. For decreasing aquifer
527 transmissivity, bank slope seems more relevant for RTD after the flood event and its
528 impact is more long-lasting. Bank slope could result in longer (near the point bar) or
529 shorter (near the cut bank) pore water RT at various times of a flood event. This
530 means that point bars with bank slopes are more conducive for river restoration (e.g.,
531 removal of dissolved organic carbon) while cut banks with bank slope may have
532 adverse effects on the groundwater quality near rivers. This is important to keep in
533 mind when assessing the influence of bank slope on biogeochemical efficiency. For
534 example, previous research indicates that the residence time of river water in the HZ
535 can control, and is often proportional to nutrient cycling (McCallum and Shanafield,
536 2016; Wondzell and Swanson, 1999; Zarnetske et al., 2011, 2012). As such, an

https://doi.org/10.5194/hess-2023-29
Preprint. Discussion started: 21 March 2023


Hydrology and Earth System Sciences
Discussions

analysis of RTD can provide valuable information on whether and where riverbank slope can induce biogeochemical hotspots and hot moments and help guide choices to be made in biogeochemical field surveys regarding location and sampling time under dynamic river stage conditions, especially when the connected aquifers have low hydraulic transmissivity.

4.2. Advantages and limitations of using a reduced 2-D model

In this study, we propose a parsimonious reduced-order, idealized horizontal 2-D model that simplifies the variation of the river-aquifer interface by using the moving boundary method to depict the displacement of SWI along a sloping riverbank. An advantage of this approach is reduced model complexity as compared to a three-dimensional model, which greatly reduces time and data requirements during model building and computational demand during simulation of HEF and especially residence time distributions. Thus, our reduced-order model acts as a first step to gain insight into the patterns of hyporheic exchange, riverbank storage and RTD in settings with more complex riverbank morphology and dynamic forcing. Future efforts should be focused on optimizing the computational method applied here and on including more detailed morphology and hydrodynamic characteristics.

It is important to note that in our simulations we assume a constant angle of bank slope along the meandering river while natural riverbanks often have non-uniform slopes which could lead to a different behavior. Thus, new conceptualizations that account for the contribution of bank slope on time-varying RTD and HZ extent can be applied to gain better understanding of a hyporheic zone, especially in cases where bank slope is small, or where the system is relatively insensitive to changes during peak flow.

In our simulations we tested the model using a range of aquifer hydraulic conductivities. Although hydraulic conductivity (or transmissivity) is a critical parameter in the quantification of exchange fluxes and RTD between the two systems

https://doi.org/10.5194/hess-2023-29
Preprint. Discussion started: 21 March 2023


Hydrology and Earth System Sciences
Discussions

564 under varying slope conditions, other parameters such as valley water head fluctuation,
565 peak flood event characteristics or larger scale groundwater head fluctuation, e.g., due
566 to changing groundwater recharge patterns have not been considered here but might
567 also impact HZ extent, RTD and river-aquifer exchange flux.
568

569 **5. Conclusions**

570 The deformed geometry method was applied to characterize the expansion and
571 contraction of hyporheic zones along sloping riverbanks, and to evaluate the impact of
572 bank slope on hyporheic exchange flux, evolution of the HZ area and RTD. To
573 achieve this, various alluvial aquifers with varying slope angles and aquifer
574 transmissivity values were simulated. Our results show that bank slope in a
575 sinuosity-driven river can have significant impact on the evolution of the hyporheic
576 zone during and after a flood event (transient flood forcing).
577 The overall findings of our work underline the need for a detailed analysis of
578 lateral hyporheic exchange flow responses to dynamic forcings (including the
579 assumption of more realistic riverbank morphology conditions). Furthermore, our
580 results show that more detailed information on bank slope (e.g., through more
581 measurements) can lead to a better understanding of hyporheic flow patterns and
582 potentially result in improved biogeochemical process understanding for real-world
583 conditions in more complex morphology and depositional environments. Several
584 conclusions can be drawn from our study:
585 1. Sloping riverbanks can increase HEF, especially when the river is connected to a
586 low-transmissivity alluvial aquifer and bank slope angles are small. However,
587 bank slope has only a minor impact on the hyporheic outflow flux.
588 2. During a flood event, the bank slope can increase the area and penetration distance
589 of the HZ into the alluvial aquifer. This effect is more pronounced and

https://doi.org/10.5194/hess-2023-29
Preprint. Discussion started: 21 March 2023


Hydrology and Earth System Sciences
Discussions

long-lasting for low-transmissivity aquifers.

3. During a flood event, the impact of bank slope on RTD is more pronounced for high transmissivity aquifers. On the contrary, the impact of bank slope on RTD for lower transmissivity aquifers is minor during the flood event, but can have a significant and long-lasting effect under post-flood conditions.
4. River sinuosity should be considered when assessing the impact of bank slope on RTD. Variable bank slope can lead to both longer and shorter RT compared to vertical riverbank conditions.
5. Bank slope has a greater impact on the residence time of hyporheic water in lower-transmissivity aquifers, thereby delaying the time of younger water discharge downstream of a meander bend, which also delays the outflow of older water upstream of that bend.

https://doi.org/10.5194/hess-2023-29
Preprint. Discussion started: 21 March 2023

Hydrology and Earth System Sciences
Discussions

Code and data availability

Additional information regarding methodology and results is provided in the supporting information (SI).

Author contributions

YL: Conceptualization, Formal analysis, Investigation
US: Conceptualization, Methodology, Writing
ZW: Funding acquisition, Software, Supervision
SK: Validation, Writing, Supervision
HL: Project administration, Supervision

Acknowledgements

This research was partially supported by the National Natural Science Foundation of China (Grant Numbers: 42272290, 41830862, and 42022018), and China Scholarship Council (CSC, 202106410042).

Competing interests

The authors declare that they have no conflict of interest.

https://doi.org/10.5194/hess-2023-29
Preprint. Discussion started: 21 March 2023

References

Bear, J., and Cheng, A. H. D.: Modeling groundwater flow and contaminant transport, Vol. 23, pp. 83, Dordrecht: Springer, 2010.

Bertrand, G., Goldscheider, N., Gobat, J.-M., and Hunkeler, D.: Review: From multi-scale conceptualization to a classification system for inland groundwater-dependent ecosystems, Hydrogeology Journal, 20, 5-25, 2012.

Boano, F., Camporeale, C., Revelli, R., and Ridolfi, L.: Sinuosity-driven hyporheic exchange in meandering rivers, Geophysical Research Letters, 33, L18406, 2006.

Boano, F., Harvey, J. W., Marion, A., and Packman, A. I., Revelli, R., Ridolfi, L., and Wörman, A.: Hyporheic flow and transport processes: Mechanisms, models, and biogeochemical implications, Reviews of Geophysics, 52, 603-679, 2014.

Boano, F., Demaria, A., Revelli, R., and Ridolfi, L.: Biogeochemical zonation due to intrameander hyporheic flow, Water Resource. Research. 46, W02511, 2010.

Boulton, A. J., Datry, T., Kasahara, T., Mutz, M., and Stanford, J. A.: Ecology and management of the hyporheic zone: Stream–groundwater interactions of running waters and their floodplains, Journal of the North American Benthological Society, 29 (1), 26-40, 2010.

Brunke, M., and Gonser, T.: The ecological significance of exchange processes between rivers and groundwater, Freshwater Biology, 37 (1), 1-33, 1997.

Cardenas, M. B.: The effect of river bend morphology on flow and timescales of surface water-groundwater exchange across pointbars, Journal of Hydrology, 362, 134-141, 2008.

Cardenas, M. B.: A model for lateral hyporheic flow based on valley slope and channel sinuosity, Water Resources Research, 45, W01501, 2009a.

Cardenas, M. B.: Stream-aquifer interactions and hyporheic exchange in gaining and losing sinuous streams, Water Resources Research, 45, W06429, 2009b.

Cardenas, M. B.: Hyporheic zone hydrologic science: A historical account of its

https://doi.org/10.5194/hess-2023-29
Preprint. Discussion started: 21 March 2023

emergence and a prospectus, Water Resources Research, 51, 3601-3616, 2015.

Cooper, H. H., and Rorabaugh, M. I.: Ground-water movements and bank storage due to flood stages in surface streams, Report of Geological Survey Water-Supply, pp. 1536-J, US Government Printing Office, Washington, United States, 1963.

Derx, J., Farnleitner, A. H., Blöschl, G., Vierheilig, J., and Blaschke, A. P.: Effects of riverbank restoration on the removal of dissolved organic carbon by soil passage during floods–A scenario analysis, Journal of Hydrology, 512, 195-205, 2014.

Doble, R. C., Crosbie, R. S., Smerdon, B. D., Peeters, L., and Cook, F. J.: Groundwater recharge from overbank floods, Water Resources Research, 48 (9), W09522, 2012a.

Doble, R., Brunner, P., McCallum, J., and Cook, P. G.: An analysis of river bank slope and unsaturated flow effects on bank storage, Ground Water, 50 (1), 77-86, 2012b.

Donea, J., A. Huerta, J.-P. Ponthot, and A. Rodriguez-Ferran.: Arbitrary Lagrangian–Eulerian methods, In Encyclopedia of Computational Mechanics, ed. E. Stein, R. de Borst, and T. J. R. Hughes, 413-434. New York: John Wiley & Sons, 2004.

Duarte, F., Gormaz, R., and Natesan, S.: Arbitrary Lagrangian–Eulerian method for Navier–Stokes equations with moving boundaries, Computer Methods in Applied Mechanics and Engineering, 193 (45-47), 4819-4836, 2004.

Fox, G. A., and Wilson, G. V.: The role of subsurface flow in hillslope and stream bank erosion: a review, Soil Science Society of America Journal, 74 (3), 717-733, 2010.

Gao, Y., Zhu, B., Zhou, P., Tang, J. L., Wang, T., and Miao, C. Y.: Effects of vegetation cover on phosphorus loss from a hillslope cropland of purple soil under simulated rainfall: a case study in China, Nutrient Cycling in Agroecosystems, 85 (3), 263-273, 2009.

Gomez-Velez, J. D., and Harvey, J. W.: A hydrogeomorphic river network model

https://doi.org/10.5194/hess-2023-29
Preprint. Discussion started: 21 March 2023


Hydrology and Earth System Sciences
Discussions

predicts where and why hyporheic exchange is important in large basins, Geophysical Research Letters, 41, 6403–6412, 2014.

Gomez, J. D., Wilson, J. L., and Cardenas, M. B.: Residence time distributions in sinuosity - driven hyporheic zones and their biogeochemical effects, Water Resources Research, 48 (9), 2012.

Gomez-Velez, J. D., Wilson, J. L., Cardenas, M. B., and Harvey, J. W.: Flow and residence times of dynamic river bank storage and sinuosity-driven hyporheic exchange, Water Resources Research, 53, 8572-8595, 2017.

Gomez-Velez, J. D., Harvey, J. W., Cardenas, M. B., and Kiel, B.: Denitrification in the Mississippi River network controlled by flow through river bedforms, Nature Geoscience, 8, 941-945, 2015.

Hagerty, D. J., Spoor, M. F., and Parola, A. C.: Near-bank impacts of river stage control, Journal of Hydraulic Engineering, 121 (2), 196-207, 1995.

Hooke, J. M.: River meandering, In E. Wohl & J. Shroder (Eds.), Treatise on geomorphology, Vol. 9, pp. 260-288, CA: Academic Press, San Diego, 2013.

Hester, E. T., and Gooseff, M. N.: Moving beyond the banks: Hyporheic restoration is fundamental to restoring ecological services and functions of streams, Environmental Science and Technology, 44 (5), 1521-1525, 2010.

Hunt, B.: An approximation for the bank storage effect, Water Resources Research, 26 (11), 2769–2775, 1990.

Kiel, B. A., Cardenas, M. B.: Lateral hyporheic exchange throughout the Mississippi River network, Nature Geoscience, 7 (6), 413-417, 2014.

Krause, S., Abbott, B. W., Baranov, V., Bernal, S., Blaen, P., Datry, T., Drummond, J., Fleckenstein, J. H., Gomez-Velez, J., Hannah, D. M., Knapp, J. L. A., Kurz, M., Lewandowski, J., Marti, E., Mendoza-Lera C., Milner, A., Packman, A., Pinay, G., Ward, A. S., Zarnetzke, J. P.: Organizational principles of hyporheic exchange flow and biogeochemical cycling in river networks across scales, Water Resources Research. 58, e2021WR029771, 2022.

https://doi.org/10.5194/hess-2023-29
Preprint. Discussion started: 21 March 2023

Krause, S., Hannah, D. M., Fleckenstein, J. H., Heppell, C. M., Pickup, R., Pinay, G., Robertson, A. L., and Wood, P. J.: Inter-disciplinary perspectives on processes in the hyporheic zone, Ecohydrology Journal. 4 (4), 481-499, 2011.

Krause, S., Lewandowski, J., Grimm, N., Hannah, D. M., Pinay, G., Turk, V., Argerich, A., Sabater, F., Fleckenstein, J., Schmidt, C., Battin, T., Pfister, L., Martí, E., Sorolla, A., Larned, S., and Turk, V.: Ecohydrological interfaces as critical hotspots for eocsystem functioning, Water Resources Research. 53, 6359-6376, 2017.

Krause, S., Tecklenburg, C., Munz, M., and Naden, E.: Streambed nitrogen cycling beyond the hyporheic zone: Flow controls on horizontal patterns and depth distribution of nitrate and dissolved oxygen in the upwelling groundwater of a lowland river, Journal of Geophysical Research: Biogeosciences, 118 (1), 54-67, 2013.

Kruegler, J., Gomez-Velez, J. D., Lautz, L. K., and Endreny, T. A.: Dynamic evapotranspiration alters hyporheic flow and residence times in the intrameander zone, Water, 12 (2), 424, 2020.

Larkin, R. G., and Sharp, J. M.: On the relationship between river-basin geomorphology, aquifer hydraulics, and groundwater flow direction in alluvial aquifers, Geological Society of America Bulletin, 104, 1608-1620, 1992.

Li, H., Boufadel, M. C., and Weaver, J. W.: Quantifying bank storage of variably saturated aquifers, Ground Water, 46 (6), 841-850, 2008.

Liang, X. Y., Zhan, H. B., and Schilling, K.: Spatiotemporal responses of groundwater flow and aquifer-river exchanges to flood events, Water Resources Research, 54 (3), 1513-1532, 2018.

Lindow, N., Fox, G. A., and Evans, R. O.: Seepage erosion in layered stream bank material, Earth Surface Processes and Landforms, 34 (12), 1693-1701, 2009.

Mayor, Á. G., Bautista, S., Small, E. E., Dixon, M., and Bellot, J.: Measurement of the connectivity of runoff source areas as determined by vegetation pattern and

https://doi.org/10.5194/hess-2023-29
Preprint. Discussion started: 21 March 2023


Hydrology and Earth System Sciences
Discussions
Open Access
EGU

729 topography: A tool for assessing potential water and soil losses in drylands,
730 Water Resources Research, 44 (10), 2008.
731 Maury, B.: Characteristics ALE method for the unsteady 3D Navier-Stokes equations
732 with a free surface, International Journal of Computational Fluid Dynamics, 6 (3),
733 175-188, 1996.
734 McCallum, J.L., P.G. Cook, P. Brunner, and D, Berhane.: Solute dynamics during
735 bank storage flows and implications for chemical baseflow separation, Water
736 Resources Research, 46: W07541, 2010.
737 McClain, M. E., Boyer, E. W., Dent, C. L., Gergel, S. E., Grimm, N. B., Groffman, P.
738 M., Hart, S. C., Harvey, J. W., Johnston, C. A., Mayorga, E., Mcdowell, W and
739 Pinay, G.: Biogeochemical hot spots and hot moments at the interface of
740 terrestrial and aquatic ecosystems, Ecosystems, 6 (4), 301-312, 2003.
741 Millar, R. G., and Quick, M. C.: Effect of bank stability on geometry of gravel rivers,
742 Journal of Hydraulic Engineering, 119 (12), 1343-1363, 1993.
743 Millington, R. J., and Quirk, J. P.: Permeability of porous solids, Transactions of the
744 Faraday Society, 57, 1200-1207, 1961.
745 Osman, A. M., and Thorne, C. R.: Riverbank stability analysis. I: Theory, Journal of
746 Hydraulic Engineering, 114 (2), 134-150, 1988.
747 Pinay, G., Peiffer, S., De Dreuzy, J. R., Krause, S., Hannah, D. M., Fleckenstein, J. H.,
748 Sebilo, M., Bishop, K., and Hubert-M, L.: Upscaling nitrogen removal capacity
749 from local hotspots to low stream orders' drainage basins, Ecosystems, 18 (6),
750 1101-1120, 2015.
751 Pohjoranta, A., and Tenno, R.: Implementing surfactant mass balance in 2D
752 FEM–ALE models, Engineering with Computers, 27 (2), 165-175, 2011.
753 Puttock, A., Macleod, C. J., Bol, R., Sessford, P., Dungait, J., and Brazier, R. E.:
754 Changes in ecosystem structure, function and hydrological connectivity control
755 water, soil and carbon losses in semi-arid grass to woody vegetation transitions,
756 Earth Surface Processes and Landforms, 38 (13), 1602-1611, 2013.

https://doi.org/10.5194/hess-2023-29
Preprint. Discussion started: 21 March 2023


Hydrology and Earth System Sciences
Discussions

757 Seminara, G.: Meanders, Journal of Fluid Mechanics, 554, 271-297, 2006.
758 Schmadel, N. M., A. S. Ward, C. S. Lowry, and J, M. Malzone.: Hyporheic exchange
759 controlled by dynamic hydrologic boundary conditions, Geophysical Research
760 Letters, 43, 4408-4417, 2016.
761 Sharp, J. M.: Limitations of bank-stopage model assumptions, Journal of Hydrology,
762 35 (1-2), 31-47, 1977.
763 Siergieiev, D., Ehlert, L., Reimann, T., Lundberg, A., and Liedl, R.: Modelling
764 hyporheic processes for regulated rivers under transient hydrological and
765 hydrogeological conditions, Hydrology and Earth System Sciences, 19 (1),
766 329-340, 2015.
767 Singh, T., Gomez-Velez, J. D., Wu, L., Wörman, A., Hannah, D. M., and Krause, S.:
768 Effects of successive peak flow events on hyporheic exchange and residence
769 times, Water Resources Research, 56 (8), e2020WR027113, 2020.
770 Singh, T., Wu, L., Gomez-Velez, J. D., Lewandowski, J., Hannah, D. M., Krause, S.:
771 Dynamic hyporheic zones: Exploring the role of peak flow events on bedform-
772 induced hyporheic exchange, Water Resources Research, 55, 218-235, 2019.
773 Stonedahl, S. H., Harvey, J. W., and Packman, A. I.: Interactions between hyporheic
774 flow produced by stream meanders, bars, and dunes, Water Resources Research,
775 49, 5450-5461, 2013.
776 Triska, F. J., Kennedy, V. C., Avanzino, R. J., Zellweger, G. W., and Bencala, K. E.:
777 Retention and transport of nutrients in a third - order stream in northwestern
778 California: Hyporheic processes, Ecology, 70 (6), 1893-1905, 1989.
779 Weatherill, J. J., Atashgahi, S., Schneidewind, U., Krause, S., Ullah, S., Cassidy, N.,
780 and Rivett, M. O.: Natural attenuation of chlorinated ethenes in hyporheic zones:
781 A review of key biogeochemical processes and in-situ transformation potential,
782 Water research, 128, 362-382, 2018.
783 Wondzell, S. M., and Swanson, F. J.: Floods, channel change, and the hyporheic zone,
784 Water Resources Research, 35 (2), 555-567, 1999.

https://doi.org/10.5194/hess-2023-29
Preprint. Discussion started: 21 March 2023

785 Wu, L., Gomez-Velez, J. D., Krause, S., Singh, T., Wörman, A., and Lewandowski, J.:
786 Impact of flow alteration and temperature variability on hyporheic exchange,
787 Water Resources Research, 56 (3), e2019WR026225, 2020.
788 Wu, L., Gomez-Velez, J. D., Krause, S., Wörman, A., Singh, T., Nützmann, G., and
789 Lewandowski, J.: How daily groundwater table drawdown affects the diel
790 rhythm of hyporheic exchange, Hydrology and Earth System Sciences, 25 (4),
791 1905-1921, 2021.
792 Wu, L., Singh, T., Gomez-Velez, J. D., Nützmann, G., Wörman, A., Krause, S., and
793 Lewandowski, J.: Impact of dynamically changing discharge on hyporheic
794 exchange processes under gaining and losing groundwater conditions, Water
795 Resources Research, 54 (12), 10-076, 2018.
796 Zarnetske, J. P., Haggerty, R., Wondzell, S. M., and Baker, M. A.: Dynamics of nitrate
797 production and removal as a function of residence time in the hyporheic zone,
798 Journal of Geophysical Research, 116, G01025, 2021.
799 Zarnetske, J. P., Haggerty, R., Wondzell, S. M., Bokil, V. A., and González-Pinzón, R.:
800 Coupled transport and reaction kinetics control the nitrate source-sink function of
801 hyporheic zones, Water Resources Research, 48, W11508, 2012.
802 Zingg, A. W.: Degree and length of land slope as it affects soil loss in run-off,
803 Agricultural Engineering, 21, 59-64, 1940.
804